

# The 1st-place Solution for CVPR 2023 OpenLane Topology in Autonomous Driving Challenge

Dongming Wu<sup>1‡</sup>, Fan Jia<sup>2</sup>, Jiahao Chang<sup>3‡</sup>, Zhuoling Li<sup>4‡</sup>, Jianjian Sun<sup>2</sup>, Chunrui Han<sup>2</sup>,  
Shuailin Li<sup>2</sup>, Yingfei Liu<sup>2</sup>, Zheng Ge<sup>2</sup>, Tiancai Wang<sup>2</sup>

<sup>1</sup> Beijing Institute of Technology, <sup>2</sup> MEGVII Technology,

<sup>3</sup> University of Science and Technology of China, <sup>4</sup> The University of Hong Kong

wudongming97@gmail.com, {jiafan, wangtiancai}@megvii.com

## Abstract

We present the 1st-place solution of OpenLane Topology in Autonomous Driving Challenge. Considering that topology reasoning is based on centerline detection and traffic element detection, we develop a multi-stage framework for high performance. Specifically, the centerline is detected by the powerful PETRv2 detector and the popular YOLOv8 is employed to detect the traffic elements. Further, we design a simple yet effective MLP-based head for topology prediction. Our method achieves 55% OLS on the OpenLaneV2 test set, surpassing the 2nd solution by 8 points.

## 1. Introduction

OpenLane Topology [6, 9] is a new perception and reasoning task for understanding 3D scene structure in autonomous driving. Given multi-view images that cover the whole panoramic field of view, it requires analyzing the relationship of perceived entities among traffic elements and centerlines. It consists of four sub-tasks, including centerline (also named lane) detection, traffic element detection, lane-lane topology, and lane-traffic topology prediction.

In this work, we present a multi-stage framework, which decouples the base detection and topology prediction tasks. The decoupling strategy is beneficial to the analysis of topology performance since topology prediction is greatly influenced by the detection performance. To this end, our solution employs the state-of-the-art 3D/2D detectors for base detection. In specific, we modify the query-based PETRv2 detector [7, 8] for 3D lane detection and employ YOLOv8 for 2D traffic detection. We also design two independent MLP-based heads for lane-lane and lane-traffic topology prediction. With simple topology heads, **our method outperforms the second-place solution by nearly 10% on Top<sub>ll</sub> and 3% on Top<sub>lt</sub>.**

<sup>‡</sup>The work is done during the internship at MEGVII Technology.

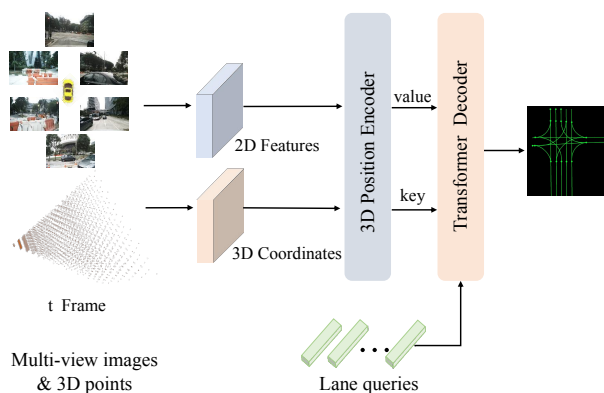


Figure 1. The overall pipeline of lane detection, which builds on PETRv2 [8] and outputs lane points.

## 2. Method

In this section, we present our model in detail. We first introduce the base model PETRv2 with several architecture modifications. Then the improved YOLOv8 using several crucial strategies is presented. Finally, we describe the MLP-based heads for topology reasoning.

### 2.1. Lane Detection

PETRv2 [7, 8] serves as a simple yet strong baseline for multi-view 3D object detection. It is developed based on DETR framework [1, 10, 11] using 3D position embedding. In specific, it encodes the position information of 3D coordinates into image features, and then uses object query to perceive the generated 3D position-aware features for end-to-end object detection in the transformer decoder. Following PETRv2, we employ the 3D position-aware features and modify the query representation for centerline detection. The overall architecture is shown in Fig. 1.

**Lane representation.** Based on the defined lane query, we aim to employ the transformer decoder to predict the 3D

- unknown
- red
- green
- yellow
- go\_straight
- turn\_left
- turn\_right
- no\_left\_turn
- no\_right\_turn
- u\_turn
- no\_u\_turn
- slight\_left
- slight\_right

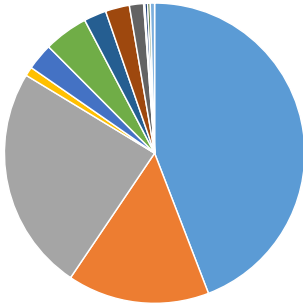


Figure 2. Category distribution on OpenLane-V2 training set.

control points of Bezier curve. Specifically, we first randomly initialize  $N$  lane queries, *i.e.*,  $Q \in \mathbb{R}^{N \times 3}$ , each of which containing a 3D point. We repeat each point by  $M$  times to fit  $M$  3D control points, *i.e.*,  $Q \in \mathbb{R}^{N \times M \times 3}$ . For each lane query, the  $M$  points are flattened and fed into the decoder, outputting the decoded features. Two independent MLPs are further used to predict the classes and control points, with respect to class head and lane head. For lane matching and loss calculation, we use Focal loss for the class head and L1 loss for the lane head. Here, the weight of Focal loss is 1.5 and the weight of L1 loss is 0.0075.

**Training strategies.** As our model has a powerful ability on scaling up, we employ different backbones for improving performance. Besides, we implement several data augmentation methods, including BDA and color gamut augmentation on HSV.

## 2.2. Traffic Element Detection

We utilize YOLOv8<sup>1</sup> as the 2D detector, which only takes the front image as input and predicts a set of 2D boxes. Based on the characteristics of the OpenlaneV2 dataset, we propose a series of strategies to improve the performance of traffic element detection.

**Strong augmentation.** Many frames in the OpenLane-V2 dataset share similar scenes and lack of foreground samples, so the detector is easy to be overfitting. We utilize strong data augmentation following YOLOX [3], including mixup, mosaic augment and color gamut augmentation on HSV. It should be introduced carefully since color augmentation may obscure the color of traffic lights, while horizontal flipping can disrupt the direction of traffic signs.

**Reweighting classification loss.** After visualizing the prediction results, we found that the main difficulty lies in the high similarity of traffic signs, rather than the localization of small-size objects, such as the attribute of “turn left”, “no turn left” and “slight left”. Meanwhile, traffic signs have relatively fixed rectangular shapes. Therefore, we choose

<sup>1</sup>The official codes we adopt in our competition solution are available at <https://github.com/ultralytics/ultralytics>.



Figure 3. The prediction results from our model on the validation set, annotated with bounding boxes, categories, and confidence.

to reweight the classification loss of these difficult samples only for foreground.

**Resampling difficult samples.** The distribution of categories in the dataset is also worth noting. Through statistics, we observe that the number of “unknown” in traffic lights accounts for almost half of all annotations, while the number of yellow lights is significantly less than that of green and red lights. The number of the leftover nine traffic signs is only 20% of the total annotations, as shown in Fig. 2. Similar to CBGS [12], we resample the frames in the dataset based on the above category statistics.

**Pseudo label learning.** We find that when the ego vehicle forward, the distant traffic elements that first appear in the video frame are usually not annotated due to their small size. Besides, there inevitably be missing annotations in both training and val sets of this dataset, which confuses the model training and leads to sub-optimal performance. The visualization in Fig. 3 shows the inference results on the validation set, where the model is only trained on the training set. It can be seen that the model has a high recall and produces an acceptable prediction for those distant small-size objects. We think the high performance detector can be used for pseudo labeling to assist the model in further training. In the ablation section, we find that using the pseudo labels on validation set significantly improves the results compared to those only on the training set.

**Test-time augmentation.** Test-Time Augmentation can steadily bring benefits during inference phase. We only adopt multi-scale testing, as complex transformations may lead to performance degradation. The scale range we adopt is selected between 0.7~1.4. The enlarged images can improve the recall of the detector for small-size objects, while the shrunk images are helpful for detecting large-size road signs on the ground in front of the ego vehicle.

## 2.3. Lane-Lane Topology

We collect the decoded features and the predicted lane coordinates from the last decoder layer. The lane coordinates are transformed into the same dimension as the de-

Method	Backbone	#Epoch	DET <sub>l</sub> (%)
Ours	ResNet50	20	18.15
Ours	VOV	20	21.01
Ours	ViT-L	20	28.11
Ours	ViT-L	48	34.16

Table 1. Ablation study of different backbones and training epochs over OpenLaneV2 validation set, in terms of DET<sub>l</sub> (%).

Method	Backbone	BDA	DET <sub>l</sub> (%)
Ours	ViT-L		34.16
Ours	ViT-L	✓	35.28

Table 2. Ablation study of BDA over OpenLaneV2 validation set, in terms of DET<sub>l</sub> (%).

coded features using an MLP, and we sum up both two kinds of features. The summed features are concatenated as the topology size of  $N \times N \times 2C$ , where  $C$  represents the feature dimension. Another MLP further transforms the topology features into a binary topology representation. We apply Focal loss to supervise the topology learning.

## 2.4. Lane-Traffic Topology

Our lane-traffic topology directly uses the traffic predictions from YOLOv8 as input. The coordinates, category, and confidence score of each box are first concatenated and then projected to  $C$ -dimensional feature vectors. Here, we denote the size of traffic features as  $T \times C$ . Therefore, the lane-traffic topology features can be formulated as  $N \times T \times C$ . With an MLP and sigmoid function, the predicted lane-traffic topology representation is also supervised by Focal loss, similar to the lane-lane topology.

## 3. Experiments

In this section, we first provide some implementation details. Then we evaluate the aforementioned parts in our method on the OpenLaneV2 validation set. The final results on the challenge will be presented as well.

### 3.1. Implementation Details

For lane detection, the size of all input images is resized to  $1550 \times 2048$ . Our model is implemented with different backbones, including ResNet50 [4], VOV [5], and ViT-L [2]. The entire network is optimized by AdamW optimizer with a learning rate of  $2e-4$ , except for the backbones using  $2e-5$ . The number of lane queries is set to 300. The model is trained with 20 epoch if not specialized.

For traffic element detection, we statistically analyze the distribution of annotations in vertical direction of the image and crop them into  $896 \times 1550$  for training efficiency. The

Method	#Epoch	lr scale	Filter empty gt	DET <sub>l</sub> (%)
YOLOv8-x	20	$\times 1$	✗	79.89
YOLOv8-x	50	$\times 1$	✗	78.98
YOLOv8-x	75	$\times 1$	✗	78.32
YOLOv8-x	20	$\times 0.5$	✗	72.45
YOLOv8-x	20	$\times 0.1$	✗	68.84
YOLOv8-x	20	$\times 1$	✓	75.90

Table 3. Ablation study of training strategies on traffic element detection over OpenLaneV2 validation set.

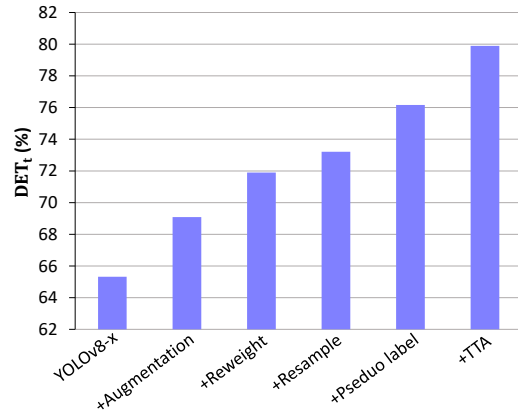


Figure 4. The contribution of each part on traffic element detection over OpenLaneV2 validation set, in terms of DET<sub>l</sub> (%).

classification loss of foreground is reweighted by 2 and the pseudo label loss is weighted by 1. For categories with a quantity ratio of less than 10%, we implement resampling based on their specific quantity, with a ratio ranging from 5 to 20 times. We load COCO-pretrained checkpoint and finetune for 20 epochs as our 2D detector baseline. And others all follow the default settings of YOLOv8-x.

For topology prediction, we freeze the 2D traffic and 3D lane detectors, and only train these MLP networks for 10 epochs. The learning rate is set to  $2e-4$ .

### 3.2. Lane Performance

We test different backbones on the OpenLane-V2 validation dataset for verifying the scaling up of our model. As shown in Table 1, it can be seen that stronger backbone brings much better performance. We also train the model using more training time, *i.e.*, 48 epochs, showing large performance improvement (+6.05% on DET<sub>l</sub>). Moreover, we investigate the impact of BDA augmentation in Table 2. Using bird’s eye data augmentation (BDA) brings about 1% performance gain of DET<sub>l</sub>.

### 3.3. Traffic Element Performance

We evaluate the aforementioned parts in our 2D traffic element detector on the OpenLane-V2 validation dataset in

DET <sub>l</sub> (%)	DET <sub>t</sub> (%)	TOP <sub>ll</sub> (%)	TOP <sub>lt</sub> (%)	OLS (%)
28.11	68.84	14.54	18.97	44.64
28.11	79.89	14.54	21.65	48.16
35.28	79.89	23.01	33.34	53.29

Table 4. The topology performance (*i.e.*, TOP<sub>ll</sub> and TOP<sub>lt</sub>) based on different lane performance DET<sub>l</sub> and traffic performance DET<sub>t</sub> on OpenLaneV2 validation set.

Rank	Name	DET <sub>l</sub>	DET <sub>t</sub>	TOP <sub>ll</sub>	TOP <sub>lt</sub>	OLS
<b>1</b>	<b>MFV</b>	0.36	<b>0.80</b>	<b>0.23</b>	<b>0.33</b>	<b>0.55</b>
2	qcraft2	0.42	0.64	0.07	0.30	0.47
3	Victory	0.22	0.72	0.13	0.23	0.45

Table 5. The final leaderboard of OpenLane Topology Challenge. We ranked 1<sup>st</sup> on the OpenlaneV2 test set.

Fig. 4. YOLOv8-x can reach a score of 65.32% on DET<sub>l</sub> without any tricks. Applying strong data augmentation has a performance improvement of 3.77%. After adjusting the classification weights, the model performance has improved to 71.90% from the previous level. Resampling solves the problem of unbalanced sample distribution and brings further improvement, while combining with pseudo labels training brings 1.31% and 2.95% improvements, respectively. Finally, we utilize Test-Time Augmentation to improve the performance to 79.89% without training models. We also explore other settings during training, as shown in Table 3. It can be seen that increasing the training epoch from 20 to 75 does not bring any performance improvement. Reducing the learning rate of finetuning stage will seriously damage performance, and samples without ground-truth annotations are still helpful for model training.

### 3.4. Topology Performance

As topology prediction heavily relies on the performance of lane detection and traffic detection, we conduct ablation experiments with different 2D traffic and 3D lane detection results, as shown in Table 4. The last row uses the best scores of detection (35.28% DET<sub>l</sub> and 79.89% DET<sub>t</sub>), while the scores of other rows (28.11% DET<sub>l</sub> and 68.84% DET<sub>t</sub>) can be seen in Table 1 and Table 3 for more details. It is obvious that the topology performance is improved with higher basic detection performance.

### 3.5. Final Result

The final result of the OpenLane Topology Challenge is shown in Table 5. Our method shows a much stronger performance (+16% DET<sub>t</sub>, +16% TOP<sub>ll</sub>, +3% TOP<sub>lt</sub>, and +8% OLS), compared to the 2<sup>nd</sup> solution. Note that the model for final submission is jointly trained on the training and validation sets of OpenlaneV2 but is not ensembled.

## References

- [1] Nicolas Carion, Francisco Massa, Gabriel Synnaeve, Nicolas Usunier, Alexander Kirillov, and Sergey Zagoruyko. End-to-end object detection with transformers. In *Computer Vision–ECCV 2020: 16th European Conference, Glasgow, UK, August 23–28, 2020, Proceedings, Part I 16*, pages 213–229. Springer, 2020. 1
- [2] Alexey Dosovitskiy, Lucas Beyer, Alexander Kolesnikov, Dirk Weissenborn, Xiaohua Zhai, Thomas Unterthiner, Mostafa Dehghani, Matthias Minderer, Georg Heigold, Sylvain Gelly, et al. An image is worth 16x16 words: Transformers for image recognition at scale. *arXiv preprint arXiv:2010.11929*, 2020. 3
- [3] Zheng Ge, Songtao Liu, Feng Wang, Zeming Li, and Jian Sun. Yolox: Exceeding yolo series in 2021. *arXiv preprint arXiv:2107.08430*, 2021. 2
- [4] Kaiming He, Xiangyu Zhang, Shaoqing Ren, and Jian Sun. Deep residual learning for image recognition. In *Proceedings of the IEEE conference on computer vision and pattern recognition*, pages 770–778, 2016. 3
- [5] Youngwan Lee, Joong-won Hwang, Sangrok Lee, Yuseok Bae, and Jongyoul Park. An energy and gpu-computation efficient backbone network for real-time object detection. In *Proceedings of the IEEE/CVF conference on computer vision and pattern recognition workshops*, 2019. 3
- [6] Tianyu Li, Li Chen, Xiangwei Geng, Huijie Wang, Yang Li, Zhenbo Liu, Shengyin Jiang, Yuting Wang, Hang Xu, Chun-jing Xu, Feng Wen, Ping Luo, Junchi Yan, Wei Zhang, Xiaogang Wang, Yu Qiao, and Hongyang Li. Topology reasoning for driving scenes. *arXiv preprint arXiv:2304.05277*, 2023. 1
- [7] Yingfei Liu, Tiancai Wang, Xiangyu Zhang, and Jian Sun. Petr: Position embedding transformation for multi-view 3d object detection. *arXiv preprint arXiv:2203.05625*, 2022. 1
- [8] Yingfei Liu, Junjie Yan, Fan Jia, Shuailin Li, Qi Gao, Tiancai Wang, Xiangyu Zhang, and Jian Sun. PetrV2: A unified framework for 3d perception from multi-camera images. *arXiv preprint arXiv:2206.01256*, 2022. 1
- [9] Huijie Wang, Zhenbo Liu, Yang Li, Tianyu Li, Li Chen, Chonghao Sima, Yuting Wang, Shengyin Jiang, Feng Wen, Hang Xu, Ping Luo, Junchi Yan, Wei Zhang, Jun Yao, Yu Qiao, and Hongyang Li. Road genome: A topology reasoning benchmark for scene understanding in autonomous driving. *arXiv preprint arXiv:2304.10440*, 2023. 1
- [10] Yingming Wang, Xiangyu Zhang, Tong Yang, and Jian Sun. Anchor detr: Query design for transformer-based detector. In *Proceedings of the AAAI conference on artificial intelligence*, volume 36, pages 2567–2575, 2022. 1
- [11] Dongming Wu, Wencheng Han, Tiancai Wang, Xingping Dong, Xiangyu Zhang, and Jianbing Shen. Referring multi-object tracking. In *Proceedings of the IEEE/CVF Conference on Computer Vision and Pattern Recognition*, pages 14633–14642, 2023. 1
- [12] Benjin Zhu, Zhengkai Jiang, Xiangxin Zhou, Zeming Li, and Gang Yu. Class-balanced grouping and sampling for point cloud 3d object detection. *arXiv preprint arXiv:1908.09492*, 2019. 2